Original scientific paper
https://doi.org/10.33180/InfMIDEM2024.102

Informacije MIDEM
Journal of Microelectronics,
Electronic Components and Materials
Vol. 54, No. 1(2024), 17 – 24

The Effect of Firing Conditions on the Characteristics of Thick-film Resistors for Temperature Sensors

Barbara Repič[1,2], Darko Belavič[1], Danjela Kuscer[1,2]

[1]Electronic Ceramics Department, Jožef Stefan Institute, Ljubljana, Slovenia
[2]Jožef Stefan International Postgraduate School, Ljubljana, Slovenia

Abstract: An integrated miniature electrochemical sensor (ES) that offers rapid, sensitive, and selective detection of chemical and biological contaminants in a variety of samples requires temperature control to work accurately. To address this, one approach is to locate temperature sensor (TS) next to the ES components. However, this integration poses a challenge as different firing processes are required for the sensor components and the TS. Commercially available thick-film materials for the realisation of TS are designed for screen printing on alumina and firing in air at 850 °C for 10 minutes. However, a key component of an ES, a carbon-based working electrode, must be fired in an oxygen-lean atmosphere. In this study, we investigated the influence of the firing atmosphere, i.e., air and argon, on the characteristics of thick-film resistors, including thickness, roughness, phase composition, resistivity, and temperature dependence. For the study, we used two commercially available thick-film pastes, NTC2114 and NTC2113, as TS with nominal sheet resistivities of 10 kΩ/sq and 1 kΩ/sq at 25 °C, respectively. Using X-ray powder diffraction analyses, we detected RuO_2 and spinel phases in the samples heated at 850 °C in air. However, when the samples were fired in argon, we detect metallic ruthenium and alloys. As a result of these changes, the resistivity of the NTC2114 and NTC2113 increased significantly. However, despite these changes, the relative resistance and the coefficient of temperature sensitivity did not vary significantly, indicating the suitability of these materials as TS. These findings have important implications for the future integration of TS into various screen-printed ES systems, fostering the design and development of systems with enhanced accuracy and reliability in temperature measurements.

Keywords: NTC, thick film, screen printing, temperature sensors, phase composition

Vpliv pogojev žganja na lastnosti debeloplastnih uporov za temperaturne

Izvleček: Miniaturni integrirani elektrokemijski senzorji omogočajo hitro, občutljivo in selektivno zaznavanje kemijskih in bioloških onesnaževalcev v različnih vzorcih. Za pridobivanje zanesljivih in natančnih meritev pa je potrebno meriti in/ali kontrolirati temperaturo vzorca na samem mestu meritve. Najbolj primerna rešitev je integracija debeloplastnega senzorja temperature v elektrokemijski senzorski sistem. Integracija predstavlja izziv, saj so materiali za izdelavo senzorskih komponent in temperaturnega senzorja drugačni in zato zahtevajo različne postopke žganja. Komercialni debeloplastni materiali za izdelavo temperaturnega senzorja so razviti za sitotisk na inertno podlago iz aluminijevega oksida in za žganje pri temperaturi 850 °C na zraku. Ključna komponenta elektrokemijskega senzorja je delovna elektroda na osnovi ogljikovih materialov, ki zahteva žganje pri povišani temperaturi v atmosferi z nizko vsebnostjo kisika. V tej študiji smo proučevali vpliv atmosfere žganja debeloplastnih materialov, zrak in argon, na debelino, hrapavost, fazno sestavo, upornost in temperaturno odvisnost upornosti. Za študijo smo uporabili paste primerne za sitotisk NTC2114 z nazivno plastno upornostjo 10 kΩ/sq in NTC2113 z nazivno plastno upornostjo 1 kΩ/sq. Rezultati so pokazali, da je po žganju na zraku v plasteh prisoten RuO_2 in spinelna faza. V plasteh, žganih pri 850 °C v argonu, teh faz nismo zasledili, pač pa smo detektirali kovinski Ru in zlitine. Posledično se je upornost plasti NTC2114 in NTC2113 močno povečala: za faktor 5 pri NTC2114 in za faktor 19 pri NTC2113. Kljub tem spremembam pa se relativna upornost in koeficient temperaturne občutljivosti (β) vzorcev nista bistveno premenila, kar kaže na primernost teh materialov za izdelavo temperaturnih senzorjev. Te ugotovitve imajo pomembno vlogo za načrtovanje in razvoj integracije temperaturnih senzorjev v druge tipe elektrokemičnih sistemov. Prispevale bodo k razvoju takih sistemov, ki omogočajo bolj natančne in zanesljive meritve temperature.

Ključne besede: NTC, debele plasti, sitotisk, temperaturni senzor, fazna sestava

** Corresponding Author's e-mail: danjela.kuscer@ijs.si*

How to cite:
B. Repič et al., "The Effect of Firing Conditions on the Characteristics of Thick-film Resistors for Temperature Sensors", Inf. Midem-J. Microelectron. Electron. Compon. Mater., Vol. 54, No. 1(2024), pp. 17–24

1 Introduction

Electrochemical sensors are a powerful tool for the rapid, sensitive, and selective detection of different types of substances in a variety of samples. They are capable of detecting chemicals such as heavy metals, pesticides, antibiotics, and food additives as well as biological contaminants such as bacteria, viruses, fungi, and associated toxins in food, air, water, and soil. As a result, these sensors are used in various areas, e.g., for food quality control, monitoring environmental conditions, and promoting industrial safety [1,2].

The electrochemical detection methods involve the interaction between the target compound, i.e., the analyte, and the sensor surface, which leads to a redox reaction. This reaction produces a detectable signal, such as a change in current, potential or impedance, which is then measured and related to the qualitative and quantitative amount of the analyte. Temperature has a major influence on electrochemical measurements. It is therefore important to measure and control the temperature when carrying out electrochemical measurements [3]. The conventional measurement is performed in an electrochemical cell consisting of a working electrode (WE), a counter electrode (CE), and a reference electrode (RE) immersed in an analyte and connected to a potentiostat that controls the electrochemical potential and measures the resulting signals. However, due to technological advances these three electrodes can be integrated onto one substrate, which has led to the development of miniaturised, low-cost and portable electrochemical sensors (ES). They offer a practical solution for the detection of different classes of compounds, especially for non-professional users in remote locations, and are suitable for real-time sensing applications. One of the most commonly used integrated ES is the planar configuration, also known as screen-printed electrode (SPE). The name is derived from its manufacturing process in which thick-film materials, i.e., pastes, are deposited onto a ceramic substrate through screen-printing technology. This approach enables the production of functional, efficient and cost-effective ES with good performance characteristics [4,5].

In conventional thick-film technology, thick-film materials are applied to alumina in paste form using the screen-printing process. These deposited thick films are dried separately at a temperature of 150 °C and then fired at a peak temperature of between 800 °C and 900 °C in an air atmosphere. For the integrated ES, the processing must be adapted to the materials used for the electrodes. The RE and CE are usually made of metals such as platinum and silver, which can withstand these processing conditions. However, the WE is often made of carbon-based materials that require a different treatment. Carbon-based materials in particular need to be fired in an inert atmosphere. This requires the investigation of technological processes and the verification of technical properties to ensure a compatible process [6].

Since the electrochemical measurements, and thus the accuracy and reliability of ES, are strongly dependent on the temperature, it is of utmost importance to measure the temperature in the immediate vicinity of the WE where the redox reactions take place. This can be achieved by integrating an additional electronic component, i.e., a temperature sensor (TS), on the alumina substrate next to the electrodes. It is most appropriate if the TS is processed with a similar technology as the other sensor components, namely by screen printing and subsequent firing. The operating principle of the TS is based on the temperature-dependent resistivity of the thick-film material, which can have a negative temperature coefficient (NTC) or positive temperature coefficient (PTC) of the resistivity [7–11].

The resistance (R) of thick-film resistors are defined by their sheet resistance (R_{SH}), their length (l) and their width (w), whereby the R_{SH} depends on the resistivity (ρ) and the thickness (t) of the screen-printed and fired layer. All these relationships are shown in the Eq. (1).

$$R = \rho \times \frac{l}{t \times w} \qquad R_{SH} = \frac{\rho}{t} \qquad R = R_{SH} \times \frac{l}{w} \quad (1)$$

Commercially available thick-film resistors usually consist of ruthenium oxide and/or bismuth ruthenate, and have a R_{SH} in decade values from 1 Ω/sq to 10 MΩ/sq. Therefore, by using materials with different R_{SH} and a different geometry of thick-film resistors, all desired different resistances can be achieved. The temperature coefficient of resistance (TCR) is described by Eq. (2), where R_1 is the resistance at temperature T_1 (usually T_1 is equal to 25 °C), and R_2 at T_2. The TCR values are below 100×10^{-6} K^{-1} for most resistors [7].

$$R_2 = R_1 \left[1 + TCR \left(T_2 - T_1 \right) \right] \quad (2)$$

Specially designed thick-film resistor materials can be used as TS. These materials are designed with a high-temperature dependence of resistivity. There are several commercially available thick-film resistor materials with high PTC or NTC of the resistivity [12,13]. Most PTC resistors have a linear characteristic of resistivity as a function of temperature (Eq. (2)), while most NTC resistors have an exponential characteristic of resistance as a function of temperature (Eq. (*3*)), where β is the coefficient of temperature sensitivity.

$$R_2 = R_1 e^{\beta\left(\frac{1}{T_1}-\frac{1}{T_2}\right)} \quad (3)$$

Commercially available PTC thick-film resistors have a R_{SH} between 10 Ω/sq and 1000 Ω/sq, and values of TCR between 1000×10^{-6} K^{-1} and 3000×10^{-6} K^{-1}. Commercially available NTC thick-film resistors have a R_{SH} between 1 kΩ/sq and 100 kΩ/sq, and values of β between -2000 K and -4000 K. Therefore, NTC sensors are more sensitive, especially at low temperatures [8]. Since in our work we investigate a relatively low and narrow temperature range up to 100 °C and a target resistance between 1 kΩ and 10 kΩ, we decided to use NTC thick-film resistors for the fabrication of TS. The NTC materials are based on the Mn-Ni-Co-O spinel phase with the addition of RuO_2 [10]. NTC pastes have been used for the realisation of temperature sensors on alumina and low temperature co-fired ceramic (LTCC) [14,15] and in microfluidic bioreactors made by multilayer LTCC technology [16].

NTC resistor has to be processed by similar technology as other sensor's components. NTC screen-printed pastes are commercially available and involve firing at a temperature of 850 °C in air atmosphere. However, the ES component, i.e., the carbon-based working electrode, requires firing in an oxygen-lean atmosphere. From our knowledge, no data is available on the processing of NTC's screen-printing pastes in such atmospheres. For compatibility purposes, the processing of NTC thick-film resistors in an oxygen-lean atmosphere needs to be studied.

In this work, we designed and processed an integrated TS using two commercially available NTC materials. The NTC pastes were screen-printed onto alumina substrate and fired at 850 °C at different conditions, namely in air for 10 min and 30 min, and in argon for 30 min. The study relates the firing conditions, thickness and phase composition of the thick-film structures to the performances of integrated sensors on an alumina substrate. The paper presents fabrication and characterization of the temperature sensors, highlighting their suitability for integration with screen-printed electrodes for electrochemical characterisation.

2 Materials and methods

2.1 Preparation of thick-film samples

Two thick-film thermistor pastes NTC2114 and NTC2113 (Ferro, King of Prussia, PA, USA) with a nominal R_{SH} of 10 kΩ/sq and 1 kΩ/sq, respectively, were used for processing temperature sensors. Thick-film resistor material (2041, DuPont Wilmington, DE, USA) with a R_{SH} of 10 kΩ/sq was used as the reference thick-film component. It was selected because it is considered to be relatively insensitive to fluctuations in the production process and enables the production of a stable and high-quality thick-film resistor [7]. The electrical interconnections and contact pads were made from a silver-based thick-film conductor (9912MM, ESL, King of Prussia, PA, USA).

The materials were screen printed on an alumina substrate (Rubalit 708S, 96% Al_2O_3, CeramTec, Plochingen, Germany) with the dimensions 24.0 mm × 10.0 mm × 0.5 mm using a screen printer (C1010, Aurel, Modigliana, Italy).

The thick-film resistors were deposited on an alumina substrate in the form of a square with dimensions of 8.0 mm x 8.0 mm for the structural investigation and of 1.1 mm x 1.1 mm with corresponding electrical interconnections for the electrical characterisations. Figure 1 shows the image of test samples, while the layout of the latter sample is shown elsewhere [17]. The screen-printed layers were dried in a dryer at 120 °C for 15 minutes and then fired under three different conditions:

i) 850 °C for 10 minutes in air with a heating and cooling rate of 33 °C/min in a chamber furnace (PEO603, ATV Technologie, Vaterstetten, Germany). The thick-film samples from pastes 2113, 2114 and 2041 processed with this profile, are referred to as 2113-10/air, 2114-10/air and 2041-10/air, respectively.
ii) 850 °C for 30 minutes in a flow of synthetic air. The samples were heated in a tube furnace at 450 °C for 1 hour at a heating rate of 2 °C/min and then heated at 850 °C for 30 minutes at a heating rate

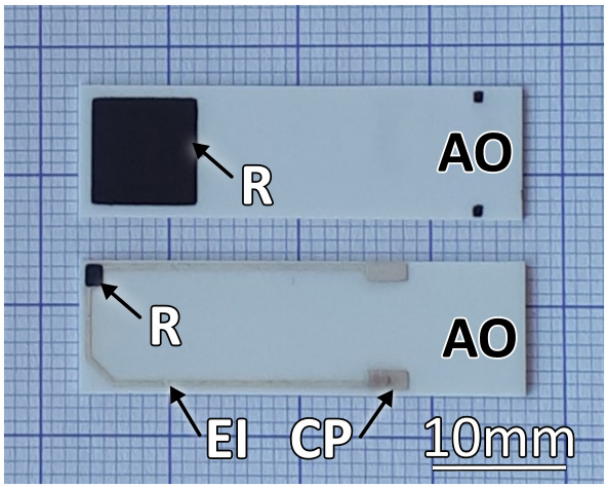

Figure 1: The photo of the test samples with dimensions 8.0 mm x 8.0 mm (above) and 1.1. mm x 1.1 mm (below), where R stands for resistor, EI for electrical interconnection, CP for contact pad, and AO for alumina substrate.

of 5 °C/min. The samples were cooled to room temperature at a cooling rate of 5 °C/min. The thick-film samples from pastes 2113, 2114 and 2041 processed according to this profile, are denoted 2113-30/air, 2114-30/air and 2041-30/air.

iii) 850 °C for 30 minutes in a flow of argon. The samples were heated in a tube furnace at 450 °C for 1 hour at a heating rate of 2 °C/min and then heated at 850 °C for 30 minutes at a heating rate of 5 °C/min. The samples were cooled to room temperature at a cooling rate of 5 °C/min. The thick-film samples from pastes 2113, 2114 and 2041 that were processed with this profile, are designated 2113-30/Ar, 2114-30/Ar and 2041-30/Ar.

2.2 Characterisation

Test samples with dimensions 8.0 mm x 8.0 mm, fired for 30 min in air and Ar, were analysed in terms of thickness and phase composition. The thickness of the samples was measured by a contact stylus profilometer (Bruker DektakXT Advanced System, Karlsruhe, Germany). The X-ray powder diffraction (XRD) patterns of the samples were collected with a benchtop Powder X-Ray Diffractometer (MiniFlex 600-C, Rigaku). Diffraction patterns were collected at room temperature in the 2θ range from 20° to 70° with a step of 0.02°and 0.24 s/step. The phases were identified using X'Pert HighScore Plus 2.1 (PANalytical) and the PDF-4 database (release 2019).

The NTC thick films and resistors with dimensions 1.1 mm x 1.1 mm, fired in air for 10 min and 30 min, and in Ar for 30 min, were characterized in an environmental chamber (VCL 7006, Voetsch Industrietechnik, Balingen-Frommern, Germany) at a constant relative humidity of about 40 % in the temperature range from -25 °C to 125 °C. The resistance of sensors and resistors was measured by a multimeter with multiplexed channels (2700, Keithley Instruments, Cleveland, Ohio, USA). The testing and measuring system was computer controlled including the acquisition of data. Resistances at 25 °C and calculated β, as key characteristics of temperature sensors, were evaluated for all samples.

3 Results and discussion

All thick-film samples fired in air and Ar for 30 min, measuring 8.0 mm x 8.0 mm, were about 30 μm thick and had a surface roughness R_a of 1 μm, regardless of the type of material and firing conditions.

XRD analysis of these samples (revealed that the samples have a high background characterised by an amorphous (glassy) phase. The amount of the glassy phase is highest in the thick film processed from 2114 paste, and lowest in 2041, regardless of the firing atmosphere. The background of the samples fired in air and argon is similar, indicating that the amount of amorphous phase for the selected sample does not vary significantly with the firing atmosphere (Figure 2, Figure 3 and Figure 4).

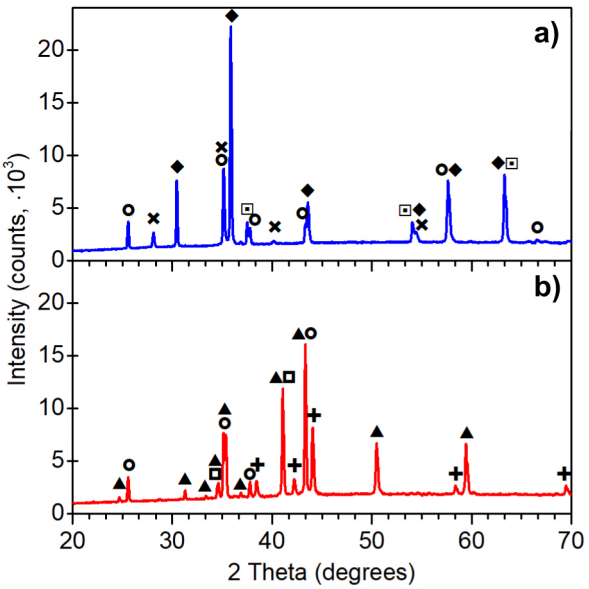

Figure 2: XRD patterns of a) 2113-30/air, and b) 2113-30/Ar. ◆: Ni-Mn-Co-O, ▲: alloys, ✖: RuO_2, ✚: Ru, ❍: Al_2O_3, ⊡: cubic SiO_2 and ◘: orthorhombic SiO_2.

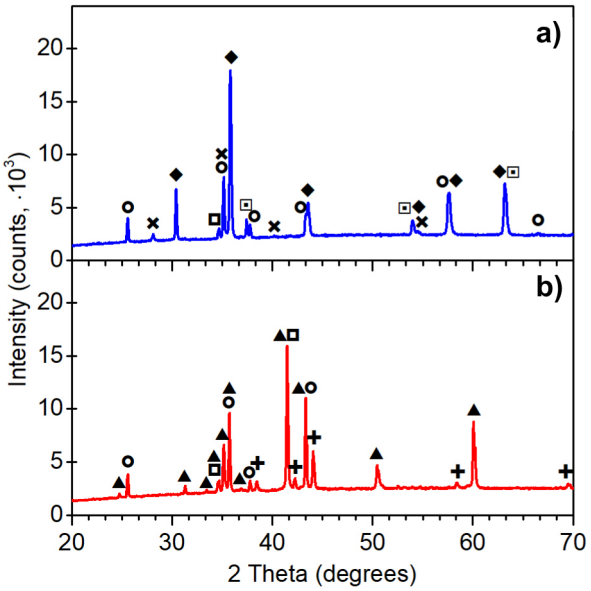

Figure 3: XRD patterns of a) 2114-30/air, and b) 2114-30/Ar. ◆: Ni-Mn-Co-O, ▲: alloys, ✖: RuO_2, ✚: Ru, ❍: Al_2O_3, ⊡: cubic SiO_2 and ◘: orthorhombic SiO_2.

The phase composition of the 2113-30/air and 2114-30/air is similar. In all the patterns we identify Ni-Mn-Co-O spinel phase (PDF 01-084-8364), RuO_2 (PDF 01-075-4303), alumina (PDF 01-075-6775) and cubic SiO_2 (PDF 01-080-4050). An additional peak at ~34 degrees is ob-

served in 2114-30/air, characterised by orthorhombic SiO_2 (PDF 04-012-8095). The phase composition of the 2041-30/air is different than those of 2113-30/air and 2114-30/air. In the pattern we identify RuO_2 (PDF 01-075-4303), $Bi_2Ru_2O_7$ (PDF 04-013-7147), alumina (PDF 01-74-6775), hexagonal SiO_2 (PDF 01-078-1257) and PbO_2 (PDF 04-020-6664). The phase composition of the air-fired samples corresponds well to the composition, reported for NTC materials and resistors [7,13].

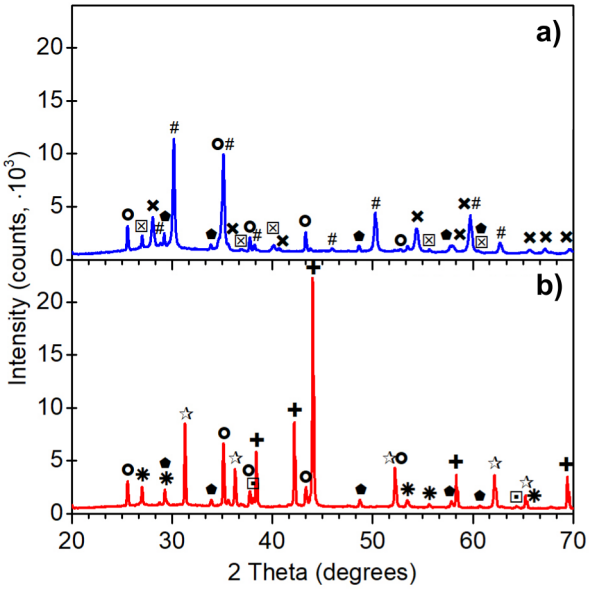

Figure 4: XRD patterns of a) 2041-30/air, and b) 2041-30/Ar. #: $Bi_2Ru_2O_7$, ✱: Bi_2O_3, ✖: RuO_2, ✚: Ru, ⬟: PbO_2, ☆: Pb_2O, ❍: Al_2O_3, ⊡: cubic SiO_2 and ☒: hexagonal SiO_2.

The samples fired in argon atmosphere have very different phase composition compared to air-fired samples. In the pattern of 2113-30/Ar and 2114-30/Ar we have not identified any spinel phase, but metallic Ru (PDF 01-071-3766), and a phase that could correspond to alloys, such as Mn-Ni (PDF 04-003-2244) and Ni-Ru (PDF 03-065-4309), Co-Mn-O rock-salt structure (PDF 04-021-8068), alumina (PDF 01-75-6775), orthorhombic SiO_2 (PDF 04-012-8095), Mn_2SiO_4 (PDF 00-009-0485) and Ni_2SiO_4 (PDF 04-014-7800). Although partial decomposition of Mn-Ni-O spinel upon heating at elevated temperature in air has been reported [19], our results showed that the spinel phase decomposed completely when the sample was heated to 850 °C in an argon atmosphere. The shift of diffraction peaks for rock-salt structure observed in 2113-30/Ar and 2114-30/Ar indicates, that its chemical composition in the two samples is different. In the 2041-30/Ar reference sample, we identify the characteristic peaks for Ru (PDF 01-071-3766), Pb_2O (PDF 00-002-0790), PbO_2 (PDF 04-020-6664), Bi_2O_3 (PDF 01-079-6675), as well as alumina (PDF 01-075-6775) and cubic SiO_2 (PDF 01-080-4050). These results clearly indicate that the spinel phase and RuO_2 decompose to metals and/or alloys when the thick-film resistors are fired in an argon at 850 °C. We expect that the resistivity of the argon-fired thick films will be very much different compared to air-fired samples, since the amount of RuO_2 and spinel phase dictate the resistivity of the NTC resistors [13,15–17].

Figure 5, Figure 6 and Figure 7 show the temperature dependences of the resistances and relative resistances for NTC2113, NTC2114 and 2041 after firing at 850 °C at

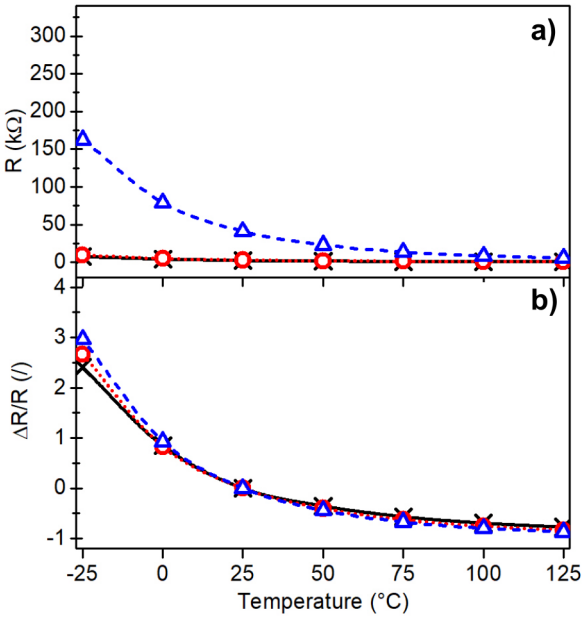

Figure 5: Resistances (a) and relative resistances (b) as a function of temperature for 2113-10/air (×), 2113-30/air (○), 2113-30/Ar (△).

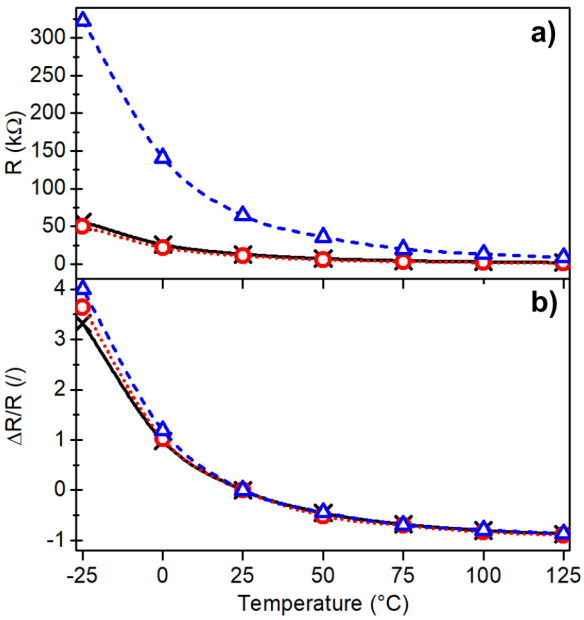

Figure 6: Resistances (a) and relative resistances (b) as a function of temperature for 2114-10/air (×), 2114-30/air (○), 2114-30/Ar (△).

different conditions. The firing of the samples in air for 10 min and 30 min resulted in similar resistances while firing in an argon significantly increases the resistance of all the samples. The R_{SH} of NTC2114 and NTC2113 increased by a factor of 5 and 19, respectively, while for the resistor 2041 it increased by a factor of 3. These changes in R_{SH} can be attributed to the absence of RuO_2 and spinel phase. However, despite these changes, the relative resistance and the coefficient of temperature sensitivity (β) did not vary significantly. The temperature range of the electrochemical sensor operation lies between 10 °C and 70 °C. In this temperature range, the maximum resistance value is around 100 kΩ for the NTC2114 and around 60 kΩ for the NTC2113.

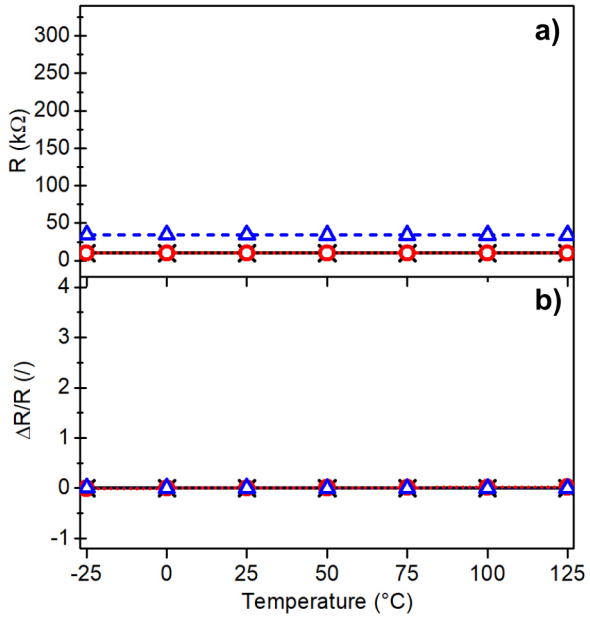

Figure 7: Resistances (a) and relative resistances (b) as a function of temperature for 2041-10/air (×), 2041-30/air (○), 2041-30/Ar (△).

Table 1 shows R_{SH} values measured at 25 °C, and β values calculated in the temperature range between 0 °C and 75 °C of the NTC2113, NTC2114 and 2041 resistors fired at different firing conditions.

The longer firing time in air has no significant influence on the R_{SH}. For samples fired for 10 and 30 minutes in air it varied for approximately +18 %, -17 %and -2 % for NTC2113, NTC2114 and 2041, respectively. On the other hand, firing in argon has a significant effect on R_{SH}. Compared to conventional firing in air for 10 minutes, the R_{SH} increased by factors of 19, 5 and 3 for NTC2113, NTC2114 and 2041, respectively.

The temperature dependence of the thick-film materials, expressed by the β, is relatively insensitive to the firing conditions. Compared to conventional firing conditions, 850 °C for 10 min in air, firing NTC2114 for 30 minutes increases the β by about 5 % in air and about 7 % in argon. The longer firing time of the NTC2113 increases the β by about 10 % and about 22 % when fired in air and argon, respectively. The thick-film resistor material 2041, which is used as a reference material, show a resistivity-independent temperature dependence.

Table 1: Sheet resistivity (R_{SH}) at 25 °C and coefficients of temperature sensitivity (β) in the temperature range between 0 °C and 75 °C of NTC2113, NTC2114 and 2041 fired at different firing conditions.

Sample	R_{SH} at 25 °C [Ω/sq]	β calculated at 0/75 °C [K]
2113-10/air	2130	-1840
2113-30/air	2522	-2019
2113-30/Ar	40937	-2250
2114-10/air	13008	-2317
2114-30/air	10822	-2441
2114-30/Ar	64507	-2480
2041-10/air	10269	1
2041-30/air	10014	16
2041-30/Ar	34394	-7

The air and Ar-fired NTC thick films have similar values of relative resistance and β, which makes them suitable for use as temperature sensors. However, when considering temperature-dependent resistivity and R_{SH}, the NTC2113 is a more appropriate material for processing temperature sensor, particularly due to easier signal conditioning.

4 Conclusions

A miniature electrochemical sensor (EC) needs temperature control for accurate operation, and one possible approach is to position temperature sensors near the EC. The EC component, the C-based working electrode, requires firing in an oxygen-lean environment, while temperature sensors are fired in air. In this study, we explored the processing of commercially available thick-film resistors, NTC2113, NTC2114, and resistor 2041, deposited on alumina substrates using screen-printing method and firing at 850 °C in air for 10 and 30 min and argon for 30 min. Obtained thick films were 30 µm thick with 1 µm surface roughness, regardless of the firing conditions, confirmed by profilometry. X-ray powder diffraction analysis showed that the films contained an amorphous phase, and its quantity did not vary significantly in air and argon for the selected samples. NTC thick films fired in air contained RuO_2, Ni-Mn-Co-O spinel phase, and minor phases, alumina, and SiO_2. The reference resistor contained RuO_2 and bismuth ruthenate as major phases, together with lead oxide, alumina, and SiO_2. We found out that argon-fired samples did not

exhibit RuO_2, spinel phase, or bismuth ruthenate, but rather metallic ruthenium and alloys. Consequently, the resistivity of the argon-fired samples was significantly higher compared to the air-fired samples. For materials fired in argon, the R_{SH} increased by a factor of 19 and 5 for NTC2113 and NTC2114, respectively. Additionally, the R_{SH} of the reference resistor increased by a factor of 3. The relative resistances and β for NTC materials were relatively unaffected by the firing atmosphere. Therefore, NTC materials show potential for use as temperature sensors. Among them, NTC2113, with its lower R_{SH}, is a more suitable material due to easier signal conditioning.

5 Acknowledgement

This work was supported by the Slovenian Research and Innovation Agency, grant numbers P2-0105, J2-3049 and PR-11483.

We thank Ivana Goričan for recording X-ray powder diffraction patterns and Mitja Jerlah for screen-printing of selected test samples.

6 References

1. T. N. Diep Trinh, K. T. L. Trinh, and N. Y. Lee, 'Microfluidic advances in food safety control', *Food Research International*, vol. 176, p. 113799, Jan. 2024, https://doi.org/10.1016/j.foodres.2023.113799.
2. A. Smart, A. Crew, R. Pemberton, G. Hughes, O. Doran, and J. P. Hart, 'Screen-printed carbon based biosensors and their applications in agri-food safety', *TrAC Trends in Analytical Chemistry*, vol. 127, p. 115898, Jun. 2020, https://doi.org/10.1016/j.trac.2020.115898.
3. R. G. Compton and C. E. Banks, *Understanding Voltammetry (Third Edition)*. World Scientific, 2018.
4. M. Li, Y.-T. Li, D.-W. Li, and Y.-T. Long, 'Recent developments and applications of screen-printed electrodes in environmental assays—A review', *Analytica Chimica Acta*, vol. 734, pp. 31–44, Jul. 2012, https://doi.org/10.1016/j.aca.2012.05.018.
5. G. Liang *et al.*, 'Development of the screen-printed electrodes: A mini review on the application for pesticide detection', *Environmental Technology & Innovation*, vol. 28, p. 102922, Nov. 2022, https://doi.org/10.1016/j.eti.2022.102922.
6. M. Prudenziati, 'Thick-film technology', *Sensors and Actuators A: Physical*, vol. 25, no. 1, pp. 227–234, Oct. 1990, https://doi.org/10.1016/0924-4247(90)87036-I.
7. M. Hrovat, Z. Samardzija, J. Holc, and D. Belavic, 'Microstructural, XRD and electrical characterization of some thick film resistors', *Journal of Materials Science: Materials in Electronics*, vol. 11, no. 3, pp. 199–208, Apr. 2000, https://doi.org/10.1023/A:1008988614598.
8. M. Hrovat, D. Belavič, J. Kita, J. Cilenšek, L. Golonka, and A. Dziedzic, 'Thick-film temperature sensors on alumina and LTCC substrates', *Journal of the European Ceramic Society*, vol. 25, no. 15, pp. 3443–3450, Oct. 2005, https://doi.org/10.1016/j.jeurceramsoc.2004.09.027.
9. A. Dziedzic, L. J. Golonka, J. Kozlowski, B. W. Licznerski, and K. Nitsch, 'Thick-film resistive temperature sensors', *Meas. Sci. Technol.*, vol. 8, no. 1, p. 78, Jan. 1997, https://doi.org/10.1088/0957-0233/8/1/011.
10. S. Jagtap, S. Rane, U. Mulik, and D. Amalnerkar, 'Thick film NTC thermistor for wide range of temperature sensing', *Microelectronics International*, vol. 24, no. 2, pp. 7–13, Jan. 2007, https://doi.org/10.1108/13565360710745539.
11. O. Aleksic and P. Nikolic, 'Recent advances in NTC thick film thermistor properties and applications', *Facta Univ Electron Energ*, vol. 30, no. 3, pp. 267–284, 2017, https://doi.org/10.2298/FUEE1703267A.
12. L. M. Sola-Laguna, P. J. Moffett, J. R. Larry, and J. Hormadaly, 'Thick film NTC thermistor series for sensor and temperature compensation application: Proceedings of the 1998 International Symposium on Microelectronics', *Proceedings of SPIE - The International Society for Optical Engineering*, vol. 3582, pp. 993–996, Dec. 1998.
13. A. H. Feingold, R. L. Wahlers, P. Amstutz, C. Huang, S. J. Stein, and J. Mazzochette, 'New Microwave Applications for Thick-film Thermistors', *Microwave Journal*, vol. 43, no. 1, pp. 90–98, 2000.
14. A. Dziedzic and E. Prociow, *Some remarks about planar thermistors*. Prague (Czech Republic): Proc. 25th Int. Spring Seminar on Electronics Technology, 2002.
15. N. Gutzeit, J. Müller, C. Reinlein, and S. Gebhardt, 'Manufacturing and Characterization of a Deformable Membrane with Integrated Temperature Sensors and Heating Structures in Low Temperature Co-fired Ceramics', *International Journal of Applied Ceramic Technology*, vol. 10, no. 3, pp. 435–442, 2013, https://doi.org/10.1111/ijac.12037.
16. H. Bartsch, F. Weise, H. Cobas, and M. R. Gongora-Rubio, 'Cost-Effective Sensor for Flow Monitoring in Biologic Microreactors', *IEEE Sensors Journal*, vol. PP, pp. 1–1, Aug. 2021, https://doi.org/10.1109/JSEN.2021.3102262.

17. D. Kuscer *et al.*, 'An advanced miniature fluidic system in multilayer ceramic technology with precise temperature and flow control for in situ pollution monitoring', *Sensors and Actuators A: Physical*, vol. 366, p. 114946, Feb. 2024, https://doi.org/10.1016/j.sna.2023.114946.
18. M. Hrovat, D. Belavič, J. Kita, J. Holc, J. Cilenšek, and S. Drnovšek, 'Thick-film NTC thermistors and LTCC materials: The dependence of the electrical and microstructural characteristics on the firing temperature', *Journal of the European Ceramic Society*, vol. 29, no. 15, pp. 3265–3271, Dec. 2009, https://doi.org/10.1016/j.jeurceramsoc.2009.05.019.
19. G. D. C. Csete de Györgyfalva and I. M. Reaney, 'Decomposition of NiMn2O4 spinel: an NTC thermistor material', *Journal of the European Ceramic Society*, vol. 21, no. 10, pp. 2145–2148, Jan. 2001, https://doi.org/10.1016/S0955-2219(01)00190-X.
20. M. Hrovat, Z. Samardžija, J. Holc, and D. Belavič, 'The development of microstructural and electrical characteristics in some thick-film resistors during firing', *Journal of Materials Science*, vol. 37, no. 11, pp. 2331–2339, Jun. 2002, https://doi.org/10.1023/A:1015385704068.
21. M. Hrovat, A. Benčan, D. Belavič, J. Holc, and G. Dražič, 'The influence of firing temperature on the electrical and microstructural characteristics of thick-film resistors for strain gauge applications', *Sensors and Actuators A: Physical*, vol. 103, no. 3, pp. 341–352, Feb. 2003, https://doi.org/10.1016/S0924-4247(02)00402-8.
22. M. Hrovat, D. Belavič, J. Holc, J. Bernard, A. Bencan, and J. Cilenšek, 'The interacions of conductive and glass phase in thick-film resistors during firing', *Informacije MIDEM*, vol. 34, pp. 7–10, Mar. 2004.

Arrived: 26. 01. 2024
Accepted: 26. 02. 2024